Pflugers Arch - Eur J Physiol (2002) 445:331–336
DOI 10.1007/s00424-002-0928-4

Joseph Santos-Sacchi

Functional motor microdomains of the outer hair cell lateral membrane

Received: 8 July 2002 / Accepted: 13 August 2002 / Published online: 6 September 2002

Abstract The outer hair cell (OHC) of the mammalian inner ear is a highly partitioned neuroepithelial cell whose lateral membrane is devoted to electromotility, a fast mechanical length change owing to the motor protein, prestin. Spatially restricted measures of prestin-derived nonlinear capacitance or gating charge, using either electrical amputation or discrete membrane mechanical deformation, were used to determine that functional variation exists within the extensive lateral membrane of the cell. This was evidenced by variation in the motor's operating voltage range and sensitivity among microdomains within the lateral membrane. That is, localized regions of the membrane evidenced Boltzmann distributions of motor charge whose midpoint voltage and slope differed from those obtained for the whole cell. These data highlight the functional independence of microdomains and imply that measured whole cell characteristics may differ from the microscopic characteristics of elementary motors.

Keywords Motility · Gating charge · Membrane capacitance

Introduction

The outer hair cell (OHC) underlies the mammal's enhanced auditory abilities [5]. It is a cell that is functionally partitioned [10, 23], possessing regions of its plasma membrane that are predominantly devoted to the tasks of forward transduction (apical membrane), reverse transduction (lateral membrane) and neurotransmission (basal membrane). The lateral membrane houses the motors of the OHC, recently identified as prestin [16, 25, 30], which are responsible for the cell's electromotility [4]. The mechanical response of the cell is mirrored by a motor-associated gating charge movement (or nonlinear capacitance) [3, 20]; the voltage dependence of the nonlinear capacitance is the same as that of electromotility [14], allowing the former to be used to assess some aspects of the cell's mechanical activity.

While the OHC lateral membrane harbors an enormous number of identical prestin molecules (approx. 7,500/μm^2 based on charge estimates [10]), the lateral membrane itself is composed of structural microdomains [15, 28]. This heterogeneity may underlie similar variability in the mechanical activity of the lateral membrane. For example, Kalinec and Kachar [15] observed local variation in the direction that microbeads moved along the surface of the electrically excited OHC. We hypothesize that the direction of forces arising from electrical stimulation of the lateral membrane results not only from cellular structural and mechanical constraints but also from intrinsic motor properties as well. Utilizing techniques to gauge motor characteristics from restricted regions (which we refer to as microdomains) of the OHC lateral membrane, we show that microdomains of molecular motors possess voltage characteristics that differ substantially from those obtained through whole cell measures.

Materials and methods

General preparation

Guinea pigs were overdosed with pentobarbital. The temporal bones were removed and OHCs were isolated from cochleas by gentle pipetting of the isolated top two turns of organ of Corti in Ca-free medium with collagenase (0.3 mg/ml). The cell-enriched supernatant was then transferred to a 700-µl perfusion chamber, and the cells were permitted to settle onto the coverglass bottom. All experiments were performed at room temperature (~23°C). A Nikon Diaphot inverted microscope with Hoffmann optics was used to observe the cells during electrical recording. A modified Lebovitz medium (NaCl, 142.2 mM; KCl, 5.37 mM; $CaCl_2$, 1.25 mM; $MgCl_2$, 1.48 mM; HEPES, 10 mM; dextrose, 5 mM;

J. Santos-Sacchi (✉)
Department of Surgery (Otolaryngology) and Section of Neurobiology, BML 244, Yale University School of Medicine, 333 Cedar St, New Haven, CT 06510, USA
e-mail: joseph.santos-sacchi@yale.edu
Tel.: +1-203-7857566
Fax: +1-203-7372502

adjusted to pH 7.2 with NaOH, and adjusted to 300 mosmol with dextrose) was used as the standard perfusion solution.

Electrical recordings

Cells were whole cell voltage-clamped with a Dagan 3900 (Dagan Corp., Minnesota) or Axopatch 200B amplifier (Axon Instruments, California). Gigohm seals were obtained at the supranuclear region of the OHC membrane prior to whole cell recording. Pipette solutions were composed of 140 mM CsCl, 10 mM EGTA, 2 mM $MgCl_2$, and 10 mM HEPES (buffered to pH 7.2 with CsOH, and adjusted to 300 mosmol with dextrose). In order to evaluate nonlinear capacitive gating currents in the absence of confounding ionic currents, the standard perfusion solution was replaced with an ionic blocking solution following seal formation (NaCl, 100 mM; tetraethylammonium, 20 mM; CsCl, 20 mM; $CoCl_2$, 2 mM; $MgCl_2$, 1.48 mM; HEPES, 10 mM; dextrose, 5 mM; adjusted to pH 7.2 with NaOH, and adjusted to 300 mosmol with dextrose [10, 20]). Data collection and analysis were performed with a Window's based whole cell voltage-clamp program, jClamp (Scisoft, Connecticut), utilizing a Digidata 1200 board (Axon Instruments). Series resistance effects on membrane voltage were corrected offline. All experiments were video taped.

Whole cell membrane capacitance was measured with two techniques: transient and AC. The former technique entailed the delivery of a stair-step voltage ranging from –160 to 120 mV, in 14 mV increments. Capacitive transients were integrated to obtain cell capacitance (C_m) measures as previously described [10]. The latter technique utilized a continuous high-resolution (2.56 ms sampling) two-sine voltage stimulus protocol (10 mV peak at both 390.6 and 781.2 Hz), with subsequent fast Fourier transform-based admittance analysis [24]. These high frequency sinusoids were superimposed on voltage ramp, step or sinusoidal stimuli. Capacitance data were fitted to the first derivative of a two-state Boltzmann function [20].

$$C_m = Q_{max}\frac{ze\ \ b}{kT(1-b)^2} + C_{lin}$$
$$b = \exp\left(\frac{-ze(V_m - V_{pkcm})}{kT}\right) \quad (1)$$

where Q_{max} is the maximum nonlinear charge moved, V_{pkcm} is voltage at peak capacitance or half-maximal nonlinear charge transfer, V_m is membrane potential, C_{lin} is linear capacitance, z is valence, e is electron charge, k is Boltzmann's constant, and T is absolute temperature.

Two methods to measure motor characteristics in restricted regions of the OHC

A double voltage-clamp technique, fully described elsewhere [10, 23], was used to electrically amputate portions of the OHC membrane. Briefly, the OHC was placed in a tight-fitting glass microchamber and simultaneously whole cell voltage-clamped (see Fig. 1, inset). The voltages within the microchamber were either the same as those delivered to the whole cell or set to ground. When set to ground, the system functions as a simple whole cell voltage clamp, where the entire cell membrane's voltage-dependent activity is evaluated. However, when the microchamber voltage command is the same as that delivered to the whole cell, only that portion of the OHC membrane outside the microchamber experiences a voltage drop, thus permitting the inspection of a restricted region of the OHC. Changing between configurations was performed instantaneously by manually switching the microchamber to ground or to the whole cell command voltage. During these experiments *C-V* functions were obtained with the transient capacitance measurement technique.

A micropipette aspiration technique was used to stress restricted regions of the OHC lateral membrane, as fully described elsewhere [26]. Briefly, patches of lateral membrane were deformed with a solution-filled glass pipette (2.5 μm diameter) fitted to a computer controlled piezoelectric driver (PZL, Burleigh Instruments, N.Y., USA). Membrane deformation near the middle of the cell was induced by movements of the driver's piston stepped in the negative direction (producing suction) of about 800 nm, controlled by the voltage magnitude delivered to the piezoelectric. Step stimuli produced motor-evoked currents that were measured as an rms response. Whole cell holding voltage was varied to obtain the current's voltage dependence. The data were fitted to Eq. 1 only to determine the voltage at peak current (V_{pkig}). During these experiments *C–V* functions were obtained with the AC capacitance measurement technique.

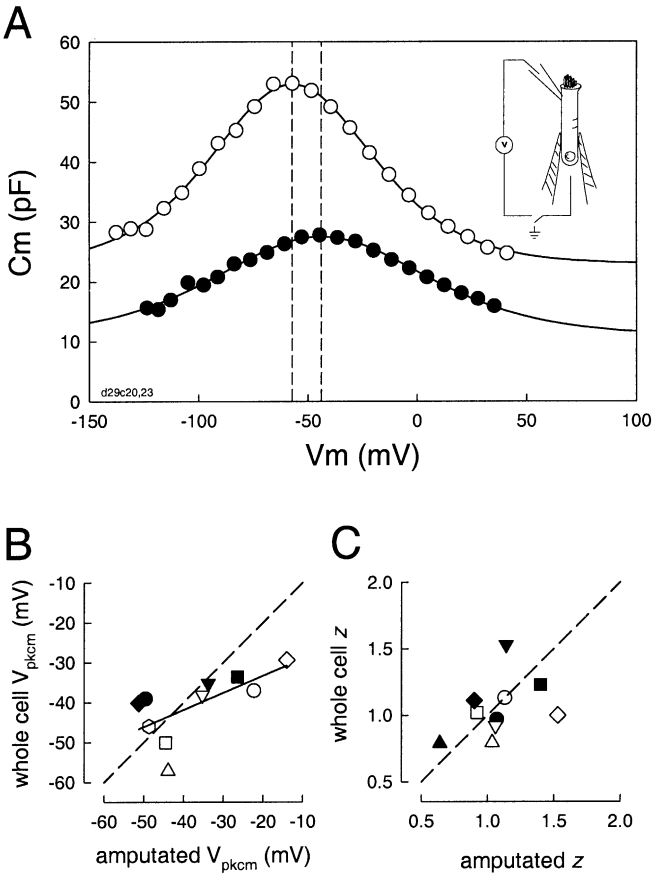

Fig. 1 **A** Membrane capacitance of outer hair cells (OHCs) before (*open circles*) and after (*closed circles*) electrical amputation in a microchamber. *Parallel dashed lines* indicate V_{pkcm} for each trace. **B** Comparison of V_{pkcm} for whole cell and amputated regions for 10 cells. *Dashed diagonal line* indicates equality. *Solid line* is linear fit to data. **C** z values for the same 10 cells. Note variability in whole cell z value

Results

For the double voltage-clamp technique, the nonlinear capacitance measured when the micro-chamber is grounded to the bath derives from all motor containing regions of the cell, since the voltage drop is impressed across the entire membrane of the cell. The capacitance measures are thus typical of whole cell conditions (Fig. 1A) and have characteristics similar to those of past reports [20].

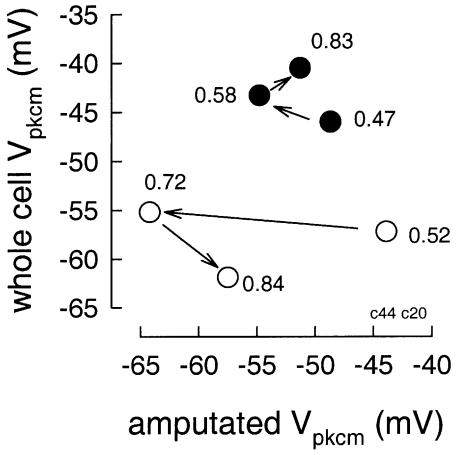

Fig. 2 Same as Fig. 1 except for two OHCs where three successive amputations were made (in the sequence of the *arrows*) following repositioning of the cell in the microchamber. Note that even though V_{pkcm} of the whole cell has shifted following repositioning, the region after amputation does not shift in parallel (neither in magnitude nor polarity), indicating its independence. The numbers indicate the degree of amputation at each measurement

Upon switching to amputation mode, the measured capacitance derives only from that portion of the cell that is outside the microchamber. The magnitude of linear as well as nonlinear capacitance is reduced (Fig. 1A), and there is an apparent shift in the V_{pkcm} to depolarized levels relative to whole cell V_{pkcm}. Figure 1B and C present V_{pkcm} data from ten cells. V_{pkcm}, which is the midpoint of the voltage range over which the motors work, differs between whole cell and the amputated region. The difference may be in the hyperpolarizing or depolarizing direction (Fig. 1B). Additionally, z, an indicator of voltage sensitivity, differs from whole cell estimates and z values can be greater or less than whole cell measures, as expected since they will sum to produce intermediate whole cell values (Fig. 1C). Pre- and post-amputation recordings were made within a few seconds of each other, in order to ensure both stationary conditions and that any experimentally induced forces, such as membrane tension imposed by the microchamber, would remain constant under each condition. Accordingly, the correlation between absolute ΔV_{pkcm} and degree of amputation was poor (r^2=0.015).

For the data just presented, the OHCs were inserted into the microchamber and remained unperturbed during the collection of pre- and post-amputation data. However, it is possible to reposition the OHC within the microchamber to obtain progressive amputations. In two cells where three successive amputations of differing magnitude were made, it was clear that whole cell V_{pkcm} changed during the repositioning (possibly due to changes in membrane tension or intracellular chloride), but that of the amputated portion tracked neither the amplitude nor the polarity of those changes (Fig. 2). For example, in one cell the initial pair of values (whole cell vs amputation) was –57.2, -43.9 mV; after repositioning for the next

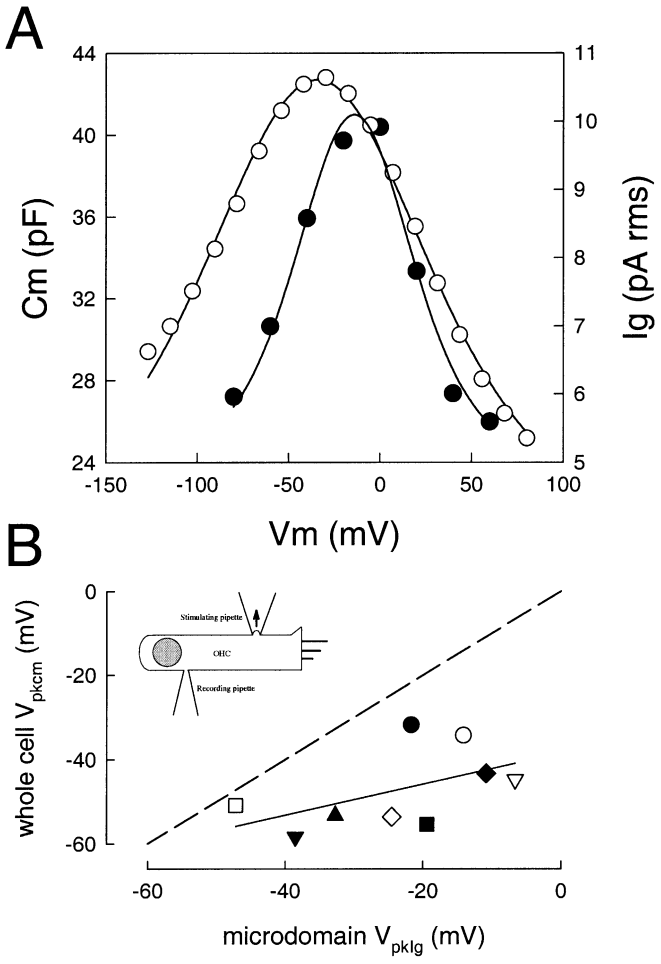

Fig. 3 **A** Whole cell capacitance (*open circles*) and microdomain stretch-induced gating currents. Note difference in voltage at peak response. **B** Comparison of voltage at peak response for 9 cells. *Dashed diagonal line* indicates equality. *Solid line* is linear fit to data. Note wide variability of V_{pkig} relative to V_{pkcm}

amputation the pair was –55.2, –64.2 mV; and after repositioning for the final amputation, the pair was –61.9, -57.5 mV. This is very strong evidence for the independent nature of OHC motor domains.

Mechanical stress of the lateral plasma membrane evokes a motor-generated displacement current (I_g) whose voltage dependence is bell-shaped like that of the cell's nonlinear capacitance (Fig. 3A). V_{pkig} is expected to be shifted to the right (in the depolarizing direction) of V_{pkcm}, since membrane stress shifts the underlying charge–voltage (Q–V) function to the right. That is, the evoked I–V function results from the difference between the shifted Q–V functions under the stressed and nonstressed conditions [9,29]. Figure 3B shows for nine cells that this expectation is met, as the data points fall to the right of the plot's dashed line of equivalence. However, the V_{pkig} of individually stressed microdomains varies widely relative to their respective whole cell V_{pkcm}. If the V_{pkcm} of the microdomains were the same as whole cell values then the two should be strictly correlated as V_{pkig} is

predicted to be midway between pre- and post-tension V_{pkcm}. Additionally, the variability is not due to differences in the degree of shift caused by the stimulus, since the correlation between peak I_g and shift magnitude was poor (r^2= 0.05). This same poor correlation also indicates that any possible variability of d.c. tension introduced by sealing the loose pipette to the membrane was not influential, since we have previously shown that steady-state tension is directly related to the magnitude of I_g [26]. If steady-state membrane tension were responsible for the variability in the shift, we might have expected a good correlation between I_g and shift. The simplest explanation is that such wide variability reflects an underlying V_{pkcm} of the stressed microdomains that differs from that of the whole cell.

Discussion

The data presented here indicate that the mechanically active lateral membrane is functionally heterogeneous, showing variability in the voltage dependence of nonlinear capacitance or motor charge movement. The gain of the OHC's electrically evoked mechanical response depends on the position of its sigmoidal displacement voltage (or corresponding bell-shaped capacitance voltage) function along the voltage axis vis-à-vis the cell's resting potential [19]. V_{pkcm}, which defines the midpoint of these functions, and therefore the OHC's voltage of maximum piezoelectric-like sensitivity, is susceptible to a variety of agents including membrane tension [9, 12, 14], resting membrane potential [24], temperature [21], phosphorylation [8, 11] and intracellular [18, 22] or extracellular [22] chloride concentration. In many cases, it has been demonstrated that these effects arise from direct action on the OHC motor protein, prestin [16, 17, 18, 25]. It should be noted that efforts were made to avoid experimentally induced changes in the parameters that describe OHC charge movement; for example, measurements of whole cell V_{pkcm} and microdomain V_{pkcm} or V_{pkig} were obtained without perturbation of the preparation and within seconds of each other, thus ensuring stationary conditions. Additionally, unequivocal evidence of microdomain independence was found when multiple amputations were made; that is, in the face of whole cell V_{pkcm} changes during repositioning cells within the microchamber, nonparallel changes (in magnitude and polarity) of microdomain V_{pkcm} were found. This could not occur if the forces that changed whole cell measures during repositioning, e.g., membrane tension or chloride concentration, were acting on a uniform population of lateral membrane motors. We conclude that while molecular sensor/motors are restricted to the expansive lateral plasma membrane, this membrane actually harbors populations of sensor/motor microdomains whose characteristics are set by local forces. Independent microdomain characteristics sum to contribute to whole cell characterizations of OHC mechanical and electrical activity.

The existence of functionally distinct microdomains, whose voltage- and tension-dependent characteristics are locally set, may have important consequences for understanding the mechanism of OHC motility. Such diversity could promote differential activation of OHC motor elements resulting in mechanical forces other than in a predominantly axial direction. For example, at a given resting membrane potential, adjacent microdomains may be contracted to different extents because mechanical gains may be different; bending or twisting movements of the OHC might be expected. Indeed, Frolenkov et al. [7] have observed bending of the OHC in an external field, but provided an explanation based on differential stimulus distributions. Whether the causes of those nonaxial motions were due to motor or stimulus characteristics is arguable; however, the likelihood that even in the face of uniform lateral membrane stimulation nonaxial forces will be evoked is strengthened by evidence from these same authors who showed lateral membrane substructure and function [15]. In addition to observing local variation in the direction that microbeads moved on the surface of the OHC, they showed by freeze etch electron microscopy that the lateral membrane presented a mosaic of microdomains with differing orientations. The mechanism that produces this mosaic is unknown, but it is possible that forces derived from the variable motor characteristics that we observed result in structural correlates. It is well known that extrinsic, local membrane forces can initiate substantial rearrangement of membrane and submembrane structure over extended time periods [27]. Alternatively, the structural differences themselves could affect motor characteristics, for example, by inducing local membrane tensions.

Our data may also relate to theories on OHC motor function, since until now it has been tacitly assumed that elementary characteristics derived from whole cell measures of motility and/or gating charge apply to all motors in the lateral membrane. Under this assumption, it has been difficult to explain the observation that a decrease in membrane tension under whole cell conditions causes a negative shift in V_{pkcm} accompanied by an increase in peak C_m [9, 14]. It has been argued that changes in peak C_m arise from membrane tension working through an anisotropic cytoskeleton or working on an anisotropic motor [9, 13]; indeed, isolated patch recordings, where tension can be applied isotropically, show only a shift in V_{pkcm} [9, 16]. Nevertheless, even in OHCs that have become spherical due to intracellular trypsin treatment, and where applied tension should be isotropic, peak C_m is altered by turgor pressure [1, 14]. We noted that motor sensitivity to membrane stress appeared greater after cortical cytoskeleton destruction with trypsin [14]. Adachi and Iwasa [1] quantified this sensitivity change by degree of V_{pkcm} shift, and found that sensitivity was about six times greater than normal, i.e., 155 mV/kPa compared to normal whole cell values of 25 mV/kPa [2, 14], which may account for their observed step-like C_m decrease [1]. Our present data may provide an alternative explanation for the effects of stress on the whole cell as opposed to

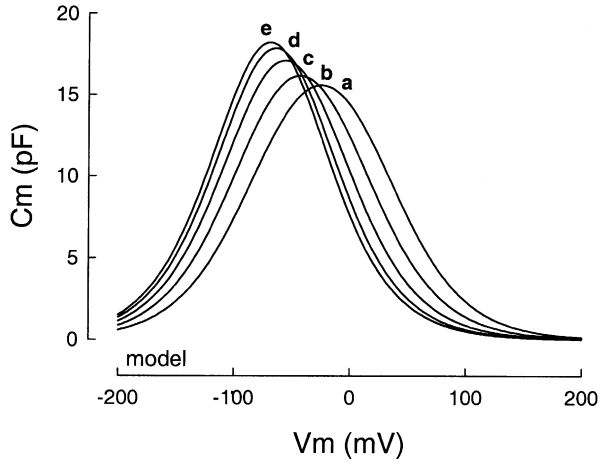

Fig. 4 Model of microdomain contributions to whole cell capacitance. In the model, each of 10 hypothetical microdomains experiences local tensions such that each V_{pkcm} is shifted 10 mV offset from each other, all of them to the right of –70 mV. The sum of these individual capacitances produces the whole cell capacitance trace *a*, and the other four traces are the result of graded decreases in tension under whole cell conditions. When tension is reduced, each microdomain V_{pkcm} shifts left towards –70 mV, the limiting V_{pkcm} [14]. As each microdomain tension is dissipated, its V_{pkcm} halts at –70 mV, and accumulates with other microdomain V_{pkcm}s producing larger peak whole cell capacitances (traces *b–d*). When all microdomain tensions are dissipated, all V_{pkcm}s reside at –70 mV and the peak capacitance is maximal (trace *e*). Q_{max} (0.25 pC) and *z* (0.75) were fixed and the same for each microdomain

patch nonlinear capacitance. First, we note that the negative shift of V_{pkcm} and increase in peak C_m during reduction of turgor pressure is asymptotic, each reaching fixed values when the OHC begins to collapse, despite continued reduction of turgor pressure [14]. The limiting negative potential is near –70 mV, close to the OHC's normal resting potential [6]. Because of this brick-wall effect, we suggest that microdomains that may have unchanging peak capacitance but variable V_{pkcm} will all shift to a single common V_{pkcm} as turgor pressure is reduced. As a result, at positive turgor pressure peak C_m will be depressed compared to negative pressure, but with increasingly negative pressures peak C_m will increase asymptotically as summation of the parallel microdomain capacitances occurs (Fig. 4). In this model we used a constant *z* of 0.66 across microdomains, yet fits of these model data to a single Boltzmann function indicate that apparent *z* is less than 0.66 initially, but increases to this level as turgor pressure is reduced. We have observed this behavior experimentally [14]. Nevertheless, the present observation that V_{pkcm} and *z* of microdomains are variable about whole cell values (Fig. 1 c) emphasizes that other forces besides tension influence the distribution of these parameters. Consequently, tension-induced changes in the form of the whole cell capacitance function may not necessarily provide insight into the microscopic characteristics of motor function. Spatially restricted patch capacitance measures, on the other hand, may provide a better sampling of microdomain characteristics.

Acknowledgements This work was supported by NIH-NIDCD grant DC00273 to J.S.S. I thank Guojie Huang, Shin Takahashi, and Margaret Mazzucco.

References

1. Adachi M, Iwasa KH (1999) Electrically driven motor in the outer hair cell: effect of a mechanical constraint. Proc Natl Acad Sci USA 96:7244–7249
2. Adachi M, Sugawara M, Iwasa KH (2000) Effect of turgor pressure on outer hair cell motility. J Acoust Soc Am 108:2299–2306
3. Ashmore JF (1990) Forward and reverse transduction in the mammalian cochlea. Neurosci Res [Suppl] 12:S39-S50
4. Brownell WE, Bader CR, Bertrand D, de RibaupierreY (1985) Evoked mechanical responses of isolated cochlear outer hair cells. Science 227:194–196
5. Dallos P (1992) The active cochlea. J Neurosci 12:4575–4585
6. Dallos P, Santos-Sacchi J, Flock A (1982) Intracellular recordings from cochlear outer hair cells. Science 218:582–584
7. Frolenkov GI, Kalinec F, Tavartkiladze GA, Kachar B (1997) Cochlear outer hair cell bending in an external electric field. Biophys J 73:1665–1672
8. Frolenkov GI, Mammano F, Belyantseva IA, Coling D, Kachar B (2000) Two distinct Ca(2+)-dependent signaling pathways regulate the motor output of cochlear outer hair cells. J Neurosci 20:5940–5948
9. Gale JE, Ashmore JF (1994) Charge displacement induced by rapid stretch in the basolateral membrane of the guinea-pig outer hair cell. Proc R Soc Lond B Biol Sci 255:243–249
10. Huang G, Santos-Sacchi J (1993) Mapping the distribution of the outer hair cell motility voltage sensor by electrical amputation. Biophys J 65:2228–2236
11. Huang G-J, Santos-Sacchi J (1993) Metabolic control of OHC function: phosphorylation and dephosphorylation agents shift the voltage dependence of motility related capacitance. ARO Midwinter Meeting Abstr 16:464
12. Iwasa KH (1993) Effect of stress on the membrane capacitance of the auditory outer hair cell. Biophys J 65:492–498
13. Iwasa KH (1996) Membrane motor in the outer hair cell of the mammalian ear. Comments. Theor Biol 4:93–114
14. Kakehata S, Santos-Sacchi J (1995) Membrane tension directly shifts voltage dependence of outer hair cell motility and associated gating charge. BiophysJ 68:2190–2197
15. Kalinec F, Kachar B (1995) Structure of the electromechanical transduction mechanism in mammalian outer hair cells. In: Flock Å, Ottoson D, Ulfendahl M (eds) Ac tive hearing. Elsevier, Oxford, pp179–191
16. Ludwig J, Oliver D, Frank G, Klocker N, Gummer AW, Fakler B (2001) Reciprocal electromechanical properties of rat prestin: the motor molecule from rat outer hair cells. Proc Natl Acad Sci USA 98:4178–4183
17. Meltzer J, Santos-Sacchi J (2001) Temperature dependence of non-linear capacitance in human embryonic kidney cells transfected with prestin, the outer hair cell motor protein. Neurosci Lett 313:141–144
18. Oliver D, He DZ, Klocker N, Ludwig J, Schulte U, Waldegger S, Ruppersberg JP, Dallos P, Fakler B (2001) Intracellular anions as the voltage sensor of prestin, the outer hair cell motor protein. Science 292:2340–2343
19. Santos-Sacchi J (1989) Asymmetry in voltage-dependent movements of isolated outer hair cells from the organ of Corti. J Neurosci 9:2954–2962
20. Santos-Sacchi J (1991) Reversible inhibition of voltage-dependent outer hair cell motility and capacitance. J Neurosci 11:3096–3110
21. Santos-Sacchi J, Huang G (1998) Temperature dependence of outer hair cell nonlinear capacitance. Hear Res 116:99–106

22. Santos-Sacchi J, Rybalchenko V (2002) Tension-dependent chloride current affects OHC capacitance. ARO Midwinter Meeting Abstr 25:255
23. Santos-Sacchi J, Huang GJ, Wu M (1997) Mapping the distribution of outer hair cell voltage-dependent conductances by electrical amputation. Biophys J 73:1424–1429
24. Santos-Sacchi J, Kakehata S, Takahashi S (1998) Effects of membrane potential on the voltage dependence of motility-related charge in outer hair cells of the guinea-pig. J Physiol (Lond) 510 (Pt 1):225–235
25. Santos-Sacchi J, Shen W, Zheng J, Dallos P (2001) Effects of membrane potential and tension on prestin, the outer hair cell lateral membrane motor protein. J Physiol (Lond) 531:661–666
26. Takahashi S, Santos-Sacchi J (2001) Non-uniform mapping of stress-induced, motility-related charge movement in the outer hair cell plasma membrane. Pflugers Arch 441:506–513
27. Veselska R, Janisch R (2001) Reaction of the skin fibroblast cytoskeleton to micromanipulation interventions. J Struct Biol 136:110–118
28. Zhang M, Kalinec F (2002) Structural microdomains in the lateral plasma membrane of cochlear outer hair cells. JARO DOI: 10.1007/s101620020016
29. Zhao HB, Santos-Sacchi J (1999) Auditory collusion and a coupled couple of outer hair cells. Nature 399:359–362
30. Zheng J, Shen W, He D, Long K, Madison L, Dallos P (2000) Prestin is the motor protein of cochlear outer hair cells. Nature 405:149–155